Neuroscience 284 (2015) 202–216

PHARMACOLOGIC RESCUE OF MOTOR AND SENSORY FUNCTION BY THE NEUROPROTECTIVE COMPOUND P7C3 FOLLOWING NEONATAL NERVE INJURY

S. W. P. KEMP,[a,b*] M. SZYNKARUK,[a] K. N. STANOULIS,[a] M. D. WOOD,[a,b] E. H. LIU,[a] M. P. WILLAND,[a,b] L. MORLOCK,[d] J. NAIDOO,[d] N. S. WILLIAMS,[d] J. M. READY,[d] T. J. MANGANO,[f] S. BEGGS,[b] M. W. SALTER,[b] T. GORDON,[a,b] A. A. PIEPER[e*†] AND G. H. BORSCHEL[a,b,c*†]

[a] *Department of Surgery, Division of Plastic and Reconstructive Surgery, The Hospital for Sick Children, Toronto, ON, Canada*

[b] *The Hospital for Sick Children Research Institute, Program in Neuroscience and Mental Health, Toronto, ON, Canada*

[c] *University of Toronto, Department of Surgery and Institute of Biomaterials and Biomedical Engineering, Toronto, ON, Canada*

[d] *Department of Biochemistry, UT Southwestern Medical Center, Dallas, TX, USA*

[e] *Departments of Psychiatry, Neurology and Veterans Affairs, Carver College of Medicine, University of Iowa, Iowa City, IA 52242, USA*

[f] *Psychoactive Drug Screening Program, University of North Carolina at Chapel Hill, Chapel Hill, NC 27599, USA*

Abstract—Nerve injuries cause pain, paralysis and numbness that can lead to major disability, and newborns often sustain nerve injuries during delivery that result in lifelong impairment. Without a pharmacologic agent to enhance functional recovery from these injuries, clinicians rely solely on surgery and rehabilitation to treat patients. Unfortunately, patient outcomes remain poor despite application of the most advanced microsurgical and rehabilitative techniques. We hypothesized that the detrimental effects of traumatic neonatal nerve injury could be mitigated with pharmacologic neuroprotection, and tested whether the novel neuroprotective agent P7C3 would block peripheral neuron cell death and enhance functional recovery in a rat neonatal nerve injury model. Administration of P7C3 after sciatic nerve crush injury doubled motor and sensory neuron survival, and also promoted axon regeneration in a dose-dependent manner. Treatment with P7C3 also enhanced behavioral and muscle functional recovery, and reversed pathological mobilization of spinal microglia after injury. Our findings suggest that the P7C3 family of neuroprotective compounds may provide a basis for the development of a new neuroprotective drug to enhance recovery following peripheral nerve injury.

Key words: neonatal nerve injury, P7C3, neuroprotection, functional recovery, microglia.

INTRODUCTION

Traumatic nerve injuries to the facial nerve or the lumbar/sacral plexus are common in newborns, and often leave patients with facial or limb paralysis (Barr et al., 2011; Malessy and Pondaag, 2011). Neonatal nerve injury occurs in 2–7.5 cases out of every 1000 live births, an incidence greater than Down's syndrome, cleft palate or spina bifida (Malessy and Pondaag, 2009; Fattah et al., 2011; Buitenhuis et al., 2012). In one form of neonatal nerve injury, obstetrical brachial plexus palsy (OBPP), the nerves of the neonate's brachial plexus are stretched or crushed during birth, sometimes to the point of rupture. OBPP occurs in about 1 of every 500 births, and often results in paralysis, numbness and chronic pain in the affected arm, shoulder and hand (Pondaag et al., 2004; Borschel and Clarke, 2009; Kozin, 2011; Pham et al., 2011). For example, more than 25% of infants with OBPP are left with permanent paralysis, numbness of the affected limb, or debilitating lifelong neuropathic pain syndromes that typically manifest in the teenage years or in early adulthood. Sadly, even with prompt and advanced surgical repair, infants with traumatic nerve injuries are often disabled for life (Squitieri et al., 2011; Phua et al., 2012). As a result, health-related quality of life for children with these types of nerve injuries and their families is poor (Firat et al., 2012; Akel et al., 2013). Clinicians rely on surgery alone to manage the severe cases, since there are no pharmacologic options presently available. The addition of an effective adjuvant medical therapy that could be administered in lieu of, or in conjunction with, state-of-the-art surgical intervention would represent a paradigm shift that would enhance the treatment of children suffering from these debilitating nerve injuries.

Peripheral nerve injury induces massive motor and sensory neuron death in both the neonatal rat (Lowrie

*Corresponding authors. Address: Department of Surgery, Division of Plastic and Reconstructive Surgery, The Hospital for Sick Children, Toronto, ON, Canada (S. W. P. Kemp, G. H. Borschel).

E-mail addresses: stevekemp.phd@gmail.com (S. W. P. Kemp), andrew-pieper@uiowa.edu (A. A. Pieper), gregory.borschel@sickkids.ca (G. H. Borschel).

† These authors contributed equally to the work.

Abbreviations: ANOVA, analysis of variance; DRG, dorsal root ganglion; EDL, extensor digitorum longus; LOD, limit of detection; LOQ, limit of quantitation; MUNE, motor unit number estimation; OBPP, obstetrical brachial plexus palsy; P3, postnatal day 3; PBS, phosphate-buffered saline.

http://dx.doi.org/10.1016/j.neuroscience.2014.10.005
0306-4522/

et al., 1987; Whiteside et al., 1998; Lewis et al., 1999; Bahadori et al., 2001) and mouse (Pollin et al., 1991; Lapper et al., 1994), as 60–70% of motoneurons in the ventral horn and sensory neurons in DRG die following nerve crush (Lowrie and Vrbova, 1984; Lowrie et al., 1987). Although the specific cause of neuron death following neonatal nerve injury is unknown, investigators have implicated glutamate-mediated cell death (Choi, 1988; Lawson and Lowrie, 1998; Mehta et al., 2013), and microglia proliferation (Morioka and Streit, 1991). Thus far, investigators have mainly sought to mitigate neonatal peripheral nerve injury in preclinical models by administering ionotropic glutamate receptor antagonists (Kapoukranidou et al., 2005; Gougoulias et al., 2007; Petsanis et al., 2012). However, these compounds fail to achieve neuronal survival rates of greater than 50% (Dekkers et al., 2001; Kalmar et al., 2002; Petsanis et al., 2012).

In the present study, we have implemented a new approach to protect these neurons from the cell death, through administration of the neuroprotective agent P7C3. This agent was originally identified through a target-agnostic *in vivo* discovery approach designed to identify new small, drug-like molecules that increase the net magnitude of hippocampal neurogenesis in mice (Pieper et al., 2010). The vast majority of newborn hippocampal neurons die before having the opportunity to integrate into hippocampal circuitry, and the discovery assay was designed to identify agents that could either enhance proliferation of these cells, or protect them from cell death. Of the compounds identified as being highly active in this assay, the P7C3-series emerged as a novel class of aminopropyl carbazoles with the ability to block cell death of neural precursor cells in the hippocampus (Pieper et al., 2010, 2014; MacMillan et al., 2011; Naidoo et al., 2013). We subsequently discovered that P7C3 compounds are also potently efficacious in blocking cell death of mature neurons located in other regions of the central nervous system as well, through testing in animal models of stress-associated depression (Walker et al., 2014), Parkinson's disease (De Jesus-Cortes et al., 2012; Naidoo et al., 2014), amyotrophic lateral sclerosis (Tesla et al., 2012) and traumatic brain injury (Blaya et al., 2014; Dutca et al., 2014; Yin et al., 2014). In all of these cases, protection of neurons from cell death by P7C3 compounds correlated with preserved neurological function. Most recently, direct activation of nicotinamide phosphoribosyltransferase, the rate-limiting enzyme in nicotinamide adenine dinucleotide salvage, has been identified as the molecular mechanism of action of the P7C3 class of compounds (Wang et al., 2014). The hope is that the P7C3-class of molecules may thus serve to facilitate development of a new class of neuroprotective drugs (Pieper et al., 2010; MacMillan et al., 2011; De Jesus-Cortes et al., 2012; Tesla et al., 2012; Asai-Coakwell et al., 2013; Blaya et al., 2013). We hypothesized that because peripheral nerve injury also induces marked neuron death, that P7C3 may rescue neurons and improve functional outcomes following nerve injury.

This represents the first time that efficacy of this series of compounds has been tested in peripheral nerve injury. We administered P7C3 to neonatal rats following sciatic nerve crush on postnatal day 3 (P3), an age at which nerve crush produces massive neuronal death (Lowrie and Vrbova, 1984; Navarrete and Vrbova, 1984). We administered P7C3 for two weeks because the vast majority of neuron death following neonatal nerve injury occurs during this time period (Lowrie et al., 1994; Aszmann et al., 2004), and we used a biologically inactive analog of P7C3, known as P7C3-S184, as a negative control. Results demonstrate that P7C3 doubled neuron survival and greatly enhanced functional recovery outcomes following nerve injury. We also show that P7C3 does not inhibit ionotropic glutamate receptors, a mechanism that has been prominently proposed for developing new treatment strategies for peripheral nerve degeneration. We also show that treatment with P7C3 reduces microglia proliferation following nerve injury to levels seen in naïve animals.

EXPERIMENTAL PROCEDURES

Neuron survival, axonal regeneration, and dose–response experiments

Animals. We used neonatal Lewis rats ($n = 42$; Charles River, Montreal, QC, Canada) at P3, weighing 8–10 g at the time of surgery. All surgical interventions were performed using inhalational anesthetic (2% Isoflurane in 98% oxygen; Halocarbon Laboratories, River Edge, NJ, USA). Rats received Metacam (0.3 mL/100 g body weight; Boehringer Ingelheim Vetmedica Inc., St. Joseph, MO, USA) for post-operative pain relief. All rats were maintained in a temperature and humidity controlled environment. Mother rats received both water and standard rat chow (Purina, Mississauga, ON, Canada) *ad libitum,*, with a 12:12-h light:dark cycle. All surgical procedures were performed aseptically under an operating microscope (Leitz, Willowdale, ON, Canada). Rats were sacrificed at study termination under deep anesthesia with Euthanyl (sodium pentobarbital, 240 mg/mL concentration, 1 mL/kg, Bimeda-MTC, Cambridge, ON, Canada) administered intracardially. The Hospital for Sick Children Laboratory Animal Services (LAS) approved these experiments, which adhered to the Canadian Council on Animal Care guidelines.

Preparation of P7C3 and P7C3-S184. P7C3 was purchased from Asinex (Moscow, Russia). Solutions were prepared according to the manufacturer's instructions. P7C3-S184 was prepared according to previously described methods (De Jesus-Cortes et al., 2012; Tesla et al., 2012).

Determination of tissue levels of P7C3 and P7C3-S184. We determined plasma and spinal cord concentrations of P7C3 to determine whether P7C3 was crossing the blood–brain barrier and entering the spinal cord. Starting three days after birth, neonatal Lewis rats were dosed with 20 mg/kg P7C3, or the same dose of

P7C3-S184 IP daily for 14 days. Six hours after the final dose, animals were sacrificed by an overdose of Euthanyl and whole blood and spinal cords were collected. Acidified citrate dextrose anticoagulant was used for blood collection, and plasma was isolated by centrifugation and stored at −80 °C until analysis. Spinal cord tissues were weighed and immediately snap frozen in liquid nitrogen prior to storage at −80 °C. Spinal cord homogenates were prepared by mincing the spinal tissue and homogenizing in a threefold volume of phosphate-buffered saline (PBS) (total volume of homogenate in ml = 4 times the mass of tissue in g). One hundred µl of plasma or tissue homogenate was mixed with 200 µl of acetonitrile containing 0.125% formic acid and 37.5 ng/ml of an internal standard, n-benzylbenzamide. The samples were vortexed for 15 s, incubated at room temperature for 10 min and centrifuged twice at 16,100*g* at 4 °C. The supernatant was saved for analysis by liquid chromatography–tandem mass spectrometry. For P7C3, the pellet was re-extracted a second time as above and the two supernatants were pooled prior to analysis. Standard curves were prepared by addition of the appropriate compound to plasma or brain homogenate. A value of threefold above the signal obtained in the blank plasma or brain homogenate was designated the limit of detection (LOD). The limit of quantitation (LOQ) was defined as the lowest concentration at which back calculation yielded a concentration within 20% of the theoretical value and above the LOD signal. The LOQ values for plasma and spinal cord were as follows: P7C3, 5 and 10 ng/ml; and P7C3-S184, 50 and 10 ng/ml. Compound levels were monitored by LC–MS/MS using an AB/Sciex (Framingham, MA, USA) 3200 Qtrap mass spectrometer coupled to a Shimadzu (Columbia, MD, USA) Prominence LC. The compounds were detected with the mass spectrometer in MRM (multiple reaction monitoring) mode by following the precursor to fragment ion transition 474.9 → 337.8 for P7C3, and 435.2 → 248.2 for P7C3-S184. The internal standard, n-benzylbenzamide, was monitored using a 212.1 → 91.1 transition.

Surgical model and experimental design. Neuron survival and axonal regeneration experiment. Our first objective was to determine whether the agent P7C3 preserved motoneurons and sensory neurons in the spinal cord following nerve peripheral nerve injury. Our second objective was to determine whether a dosing regimen existed at which neuron survival was maximal. Seven surgical groups were used in the neuron survival dose–response study (42 rat pups, age three days: *n* = six per group): (1) P7C3 (20 mg/kg/d); (2) P7C3 (10 mg/kg/d); (3) P7C3 (5 mg/kg/d); (4) P7C3 (1 mg/kg/d); (5) vehicle control; (6) inactive analog of P7C3 control (P7C3-S184), and (7) naïve animals, with no nerve injury. A mid-thigh incision was made in all rats; in those receiving a nerve injury, the right sciatic nerve was crushed with a standard #5 jewelers forceps for 30 s, producing an axonotmetic or Sunderland grade 2 injury (Bridge et al., 1994). Following the nerve crush, an 8-0 stitch was sutured into the epineurium in order to landmark where the crush site was at tissue harvest. Following surgery, all rats were returned to their home cages with their mothers, and were dosed daily for 2 weeks.

Retrograde labeling of spinal motoneurons and dorsal root ganglion (DRG) cells

In order to assess motor and sensory neuronal survival, retrograde labeling was performed one month following the initial surgery, as previously described (Kemp et al., 2013). The experimental design is shown in Fig. 1. Briefly, the right sciatic nerve was re-exposed at mid-thigh level and transected 5 mm proximal to the original crush site, a site which is quite proximal to the original injury. The proximal sciatic nerve stump was immediately placed in a silicone well containing a 4% solution of FluoroGold (FG: Fluorochrome LLC, Denver, CO, USA) in sterile saline for one hour. Silicone wells were then removed and the application site was rinsed three times with sterile saline solution. Incisions were subsequently closed and all animals were allowed to recover for 7 days. Rats were then deeply anesthetized with Euthanyl and perfused with 0.9% saline and cold 4% paraformaldehyde in PBS prior to harvesting the lumbar region (L3–L6) of the spinal cord and L4–L5 of the DRG. Both the spinal cords and DRGs were post-fixed in 4% paraformaldehyde, cryoprotected in 20% sucrose and then embedded in optimal cutting temperature compound (OCT: Sakura Fine Technical Co., Torrance, CA, USA). Subsequently, either 30-µm (spinal cord), or 20-µm (DRG) serial longitudinal sections were cut with a cryostat (Leica Microsystems Inc., Concord, ON, Canada) at −22 °C and mounted onto Superfrost slides (Fisher Scientific, Ottawa, ON, Canada). We initiated counting with the first positively labeled neuronal cell body for both spinal cord and DRG sections. For analysis, we counted every positively labeled neuron in the ventral horn of each spinal cord section and the positively labeled neurons in every fifth DRG longitudinal section, which were counted on a fluorescent microscope with a 20× objective (200× overall magnification; Leica). This procedure is identical to the retrograde counting procedure previously published in our lab (Wood et al., 2011). A blinded observer performed all counts, which were corrected for split cells using a correction factor, as detailed previously (Abercrombie, 1946).

Histomorphometric analysis

During the retrograde labeling procedure, a 5-mm sciatic nerve sample 5 mm distal to the original crush site was harvested for nerve histomorphometry, a site which is quite distal to the original injury (Fig. 1). Histomorphological analysis was conducted in accordance with previously established guidelines. Nerve samples were fixed in 2.5% glutaraldehyde buffered in 0.025 M cacodylate overnight, washed, and then stored in 0.15 M cacodylate buffer. Samples were subsequently fixed in 2% osmium tetraoxide, washed in graded alcohols, and embedded in EPON. Transverse sections at 1-µm thickness were made through the center of the sample and stained with toluidine blue.

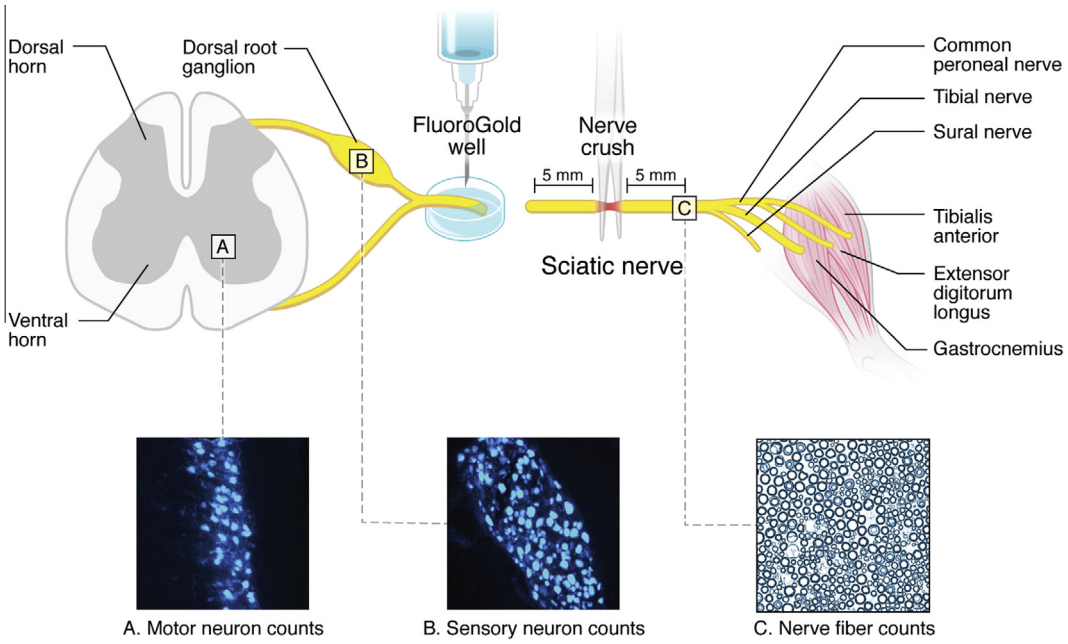

Fig. 1. Method of assessing neuron survival and regeneration after nerve injury. After sciatic nerve crush injury on postnatal day 3, treatment with test compounds began immediately and continued daily for two weeks. One month following crush injury, the sciatic nerve was transected 5 mm proximal to the original crush injury. The resulting proximal end was placed in a well containing 4% FluoroGold dye for 1 h. The dye was retrogradely transported into the cell bodies of the surviving sciatic motor and sensory neurons within the ventral horn of the spinal cord and the dorsal root ganglion, respectively. Axonal regeneration was assessed by harvesting a section of nerve 5 mm distal to the original crush site and counting the regenerated nerve fibers.

With the observer blinded to the identity of the experimental groups, cross-sections of the nerve were photographed under light microscopy (1000×). Photographs were taken of the entire cross-sectional area of the nerve, and each individual section was analyzed using Image Pro Plus software (MediaCybernetics, Bethesda, MD, USA) as previously described (Kemp et al., 2009). Nerve segmentation was done using MATLAB (The Mathworks Inc., Natick, MA, USA), and the counting procedure was identical to that previously detailed (More et al., 2011). We assessed: (1) total number of myelinated fibers; (2) g-ratio; (3) myelin thickness, and; (4) fiber diameter distribution.

Statistical analysis

The normality of the data was first assessed using the Kolmogorov–Smirnov test ($p > 0.05$). Data were analyzed using a one-way analysis of variance (ANOVA), with post hoc Bonferroni correction applied as appropriate. Repeated measures ANOVA was used for all behavioral tests. Statistical significance was accepted at the level of $p < 0.05$; all data are expressed as the mean + SEM.

Behavioral and functional experiments

Animals. Neonatal Lewis rats ($n = 18$; Charles River, Montreal, QC, Canada) at P3, weighing 8–10 g at the time of surgery were used in this study, and all surgical procedures were carried out as described above. These animals were a separate cohort from those used in the dose–response studies.

Surgical model and experimental design. Behavioral experiment. Our objective was to determine whether the optimal P7C3 dose of 20 mg/kg would enhance sensorimotor behavior following injury.

We compared three groups in the functional recovery study (18 rats; $n = 6$ rats per group): (1) P7C3 (20 mg/kg/d); (2) vehicle control, and; (3) naïve animals. Rats in groups 1 and 2 underwent a right sciatic nerve crush at P3 as previously described above. Following surgery, all animals were returned to their home cage with their mothers. Rat pups were then dosed for 2 weeks. One month following the initial surgery, all rats were trained on overground locomotion, skilled locomotor, and sensory behavioral tests. Following a one-week training period, rats were serially evaluated over the ensuing two months with weekly behavioral testing sessions.

Overground locomotion: walking track. We assessed overground, flat-surface locomotion by analyzing rat hindlimb footprints in a walking track apparatus (Monte-Raso et al., 2008). The walking track apparatus was constructed from clear Plexiglas (1 m long, 20 cm high, 8.5 cm wide). White paper lined the bottom of the apparatus, and rats were trained to walk the length of the apparatus after inking their hindpaws with black finger paint (Crayola, Lindsay, ON, Canada). All animals were videotaped in order to assess the velocity of each animal's run post hoc. The sciatic functional index (SFI) score was

determined as previously outlined (de Medinaceliet al., 1982; Bain et al., 1989).

Skilled locomotion: tapered beam. Rats were trained for one week to cross a horizontally elevated tapered beam (100 cm high; 80 × 5 cm length) one month following the initial surgery (Alant et al., 2011; Kemp et al., 2011). Five satisfactory runs were used for each animal at each time point, with a satisfactory run being defined as the animal traveling across the beam uninterrupted with a steady gait and constant velocity. The rats' performance was video-recorded and subsequently analyzed frame-by-frame at 60 Hz in a blinded fashion by a trained observer. The number of times that a rat slipped off the ledge with the affected right hindlimb was recorded, and the number of slips was normalized to the total number of steps taken during each run. Complete slips off the ledge were defined and scored as a full slip (given a score of 1). Partial slips from the elevated beam (limbs touching the side of the beam without the rat fully falling off) were defined and scored as a half slip (given a score of 0.5). Complete and partial slips were added, and a hindlimb slip ratio (%) was subsequently calculated as the number of right hindlimb slips per total number of right hindlimb steps × 100%.

Skilled locomotion: ladder rung. We trained rats to cross a horizontally placed ladder from a neutral cage to reach their home cage for a period of one week (Kemp et al., 2010). The ladder apparatus consisted of sidewalls made of clear Plexiglas (1 m long, 20 cm high) and metal rungs (3-mm diameter) that were inserted 1 cm from the bottom of the Plexiglas, and could be separated by 1-cm increments. During testing, an irregular pattern of the rungs was changed between trials in order to prevent the rats from learning the spacing pattern, as previously described (Metz and Whishaw, 2002). A single run was deemed satisfactory if the animal traveled across the beam uninterrupted at a constant velocity, and 10 satisfactory runs from each animal were used to evaluate their performance. A mirror was placed at a 45° angle below the ladder so that the rats could be video recorded from both a lateral and a ventral view. Steps with the right hindlimb were scored as either a correct or an incorrect step. Incorrect steps consisted of steps that involved a total miss of the rung or a deep slip from the rung, similar to a score of 0 or 1 (Metz and Whishaw, 2002). A slip ratio (%) was then calculated as the number of right hindlimb slips per total number of right hindlimb steps × 100%.

Sensory recovery: von Frey test. The von Frey test was used to measure recovery of cutaneous footpad sensation following nerve injury (Kemp et al., 2011). This test uses a series of filaments of different size, each delivering a stimulus of progressively varying pressures, with the larger diameter filaments exerting greater pressure (Vergnolle et al., 2001; Hasegawa et al., 2010; Wen et al., 2010). Nine von Frey filaments ranging from 0.31 to 0.81 mm in diameter with marking forces of 2.04–125.89 g (forces were verified prior to use on a standard weight scale) were applied to the rat's right hindpaw in ascending sequential order of size. Each filament was applied until a withdrawal response was elicited three out of five times by the same filament, and accompanied by either vocalization or a paw lick. All rats were tested at baseline, and then subsequently every other week following surgery beginning at 1 week post-surgery.

Muscle force analysis. Isometric force produced by the extensor digitorum longus (EDL) muscle in response to stimulation of the sciatic nerve was measured at 12 weeks. All rats were anesthetized and the sciatic nerve was isolated. Animals were subsequently placed in a custom-designed force measurement jig (Red Rock Inc, St. Louis, MO, USA) where the leg was immobilized by anchoring the femoral condyles. The stainless steel S-hook attached to the EDL muscle was connected to a 2-N-thin film load cell (S100, Strain Measurement Devices Inc., Meriden, CT, USA). Cathodic, monophasic electrical impulses (duration = 200 μs, frequency = 0–500 Hz, amplitude = 0–3 V) were generated using a single-channel isolated pulse stimulator (Model 2100, A-M Systems Inc., Carlsborg, WA, USA) and delivered to the sciatic nerve proximal to the trifurcation via bipolar silver wire electrodes. MATLAB software (The Mathworks Inc., Natick, MA, USA) calculated both the passive and active force for each recorded force trace (Red Rock Inc., St. Louis, MO, USA).

Isometric twitch contractions measured using the custom force recording system were utilized to determine the optimal stimulus amplitude (A_o) and optimal muscle length (L_o) for isometric force production in the EDL muscle. Stimulus amplitude was incrementally increased while muscle length was held constant to determine the largest active force (A_o). Single twitch contractions were recorded, and peak twitch force (F_t) was calculated. Tetanic contractions were recorded by delivering 300 μs bursts of increasing frequency (5–200 Hz) to the sciatic nerve, while allowing two-minute periods between stimuli for muscle recovery. Maximum isometric tetanic force (F_o) was calculated from the active force plateau.

Motor unit number estimation (MUNE)

In order to estimate the number of motor units (each motor neuron and the skeletal muscle fibers innervated by its axon) in the EDL, we used a modified version of the mechanical MUNE method (McComas et al., 1971). This method overcomes the problem of alternation (motor units recruited in numerous combinations by stimulation of a motor nerve) by calculating the average of 10 randomly chosen motor unit forces produced by incremental force increases at different stimulus amplitudes instead of counting incremental increases in muscle twitch force (Major and Jones, 2005; Hegedus et al., 2007; Major et al., 2007).

Wet muscle mass

Immediately following muscle force and MUNE analysis, the tibialis anterior, EDL), soleus, and the medial and lateral gastrocnemius muscles were harvested from

both the experimental and non-injured control hindlimb. A muscle mass ratio was then calculated (muscle mass ratio = mass of experimental muscle/mass of contralateral muscle).

Mechanism experiments

K_i determinations for glutamate subtype receptor binding. K_i determinations were provided by the National Institute of Mental Health's Psychoactive Drug Screening Program, Contract # HHSN-271-2008-00025-C (NIMH PDSP). The NIMH PDSP is directed by Bryan L. Roth MD, PhD at the University of North Carolina at Chapel Hill and Project Officer Jamie Driscol at NIMH, Bethesda MD, USA. For experimental details please refer to the PDSP web site http://pdsp.med.unc.edu/ and click on "Binding Assay" on the menu bar.

Animals. For the microglia experiments, neonatal Lewis rats (n = 18; Charles River, Montreal, QC) at P3, weighing 8–10 g at the time of surgery were used in this study, and all surgical procedures were carried out exactly as was done in the dose–response study. These animals were a separate cohort from those used in the previous two experiments.

Surgical model and experimental design. Mechanism experiment. Our objective was to determine whether P7C3 attenuated activated microglia proliferation following neonatal nerve injury.

We compared three groups in the microglia proliferation study (18 rats; n = 6 rats per group): (1) P7C3 (20 mg/kg); (2) vehicle control, and; (3) naïve animals. Rats in Groups 1 and 2 underwent a right sciatic nerve crush at P3 as previously described. Following surgery, all animals were returned to their home cage with their mothers. Rat pups were then dosed for 2 weeks.

Immunohistochemistry. At 1 month, all animals were terminally anesthetized with intraperitoneal Euthanyl (100 mg/kg) and transcardially perfused with heparinized saline, followed by 4% paraformaldehyde for immunohistochemical detection of microglia as previously described (Beggs and Salter, 2007). Briefly, L4 and L5 spinal segments were identified, removed, and post-fixed in 10% formalin overnight at 4^0C. Following cryoprotection in 30% sucrose, the cords were cut into 50-μm free-floating sections, and washed in phosphate-buffered saline prior to and between subsequent steps. Tissue was blocked for 1 h at room temperature (10% normal donkey serum and 0.3% Triton in phosphate-buffered saline), incubated in rabbit anti-Iba1 antibody (microglia marker; 1:2000; Wako) and mouse anti-NeuN (neuronal marker; 1:2000: Millipore) in phosphate-buffered saline with 3% normal donkey serum and 0.3% Triton for 48 h at 4 °C, followed by either Cy2 or Cy3 secondaries (1:1000; Sigma Aldrich). Finally, sections were mounted on silane-coated slides (Sigma Aldrich), allowed to dry and coverslipped with Gelmount (Sigma–Aldrich).

Spinal cord sections were imaged using a Zeiss confocal microscope and gray scales were adjusted using Adobe CS5 software. Data from 5 sections per animal were grouped together to give a mean value for each animal. To assess the spatial distribution of Iba-1 immunoreactivity, the area of microglial proliferation in both the dorsal and ventral horns was quantified using Volocity software (Improvision, PerkinElmer).

RESULTS

P7C3 enhanced motor and sensory neuron survival following neonatal sciatic nerve crush injury

One month following sciatic nerve crush injury, neuron survival was assessed by retrograde FluoroGold (FG) labeling of neuronal cell bodies (1). This technique allows quantification of surviving motor and sensory neurons with fluorescence microscopy (Naumann et al., 2000). Surviving FG-labeled motoneurons in the ventral horn are shown in Fig. 2A–F, demonstrating that P7C3 rescued motoneurons in a dose-dependent manner (Fig. 2G; [$F_{(6,35)}$ = 17.87, p < 0.01]). At the highest dose tested (20 mg/kg/d), treatment with P7C3 preserved motoneurons to a level approaching that of naïve animals. Administration of P7C3 at 10 mg/kg/d also enhanced motoneuron survival compared with vehicle, but lower doses of P7C3 did not. Importantly, the structurally related but inactive analog of P7C3, known as P7C3-S184 (De Jesus-Cortes et al., 2012), imparted no protection when administered at the same dose of 20 mg/kg/d (Fig. 2G). P7C3 at 20 mg/kg/d also significantly enhanced survival of sensory DRG neurons after injury to levels that closely approximated naïve animals (Fig. 2H) [$F_{(6,35)}$ = 12.09, p < 0.01]. Liquid chromatography–tandem mass spectroscopy analysis of spinal cord and blood showed that both P7C3 and P7C3-S184 accumulated to similar levels in these tissues after peripheral administration (data not shown). At no time during the study did we observe any abnormal behavior with animals administered P7C3, and no toxicity following P7C3 administration (data not shown).

P7C3 enhanced axonal regeneration

To assess whether P7C3-mediated neuronal survival was associated with nerve regeneration distal to the site of injury, we quantified the number and size of regenerated myelinated nerve fibers, per established protocol (Raimondo et al., 2009). Rats receiving P7C3 at 20 mg/kg/d regenerated more myelinated fibers than did rats receiving lower doses of P7C3 or vehicle [$F_{(6,27)}$ = 12.19, p < 0.01; Fig. 3A]. Although the fiber diameter distribution of normal nerves is bimodal, regenerating nerves after nerve injury typically display a unimodal distribution (Jenq and Coggeshall, 1985). Notably, however, a bimodal distribution of regenerating myelinated axons was observed in P7C3-treated animals after injury, suggesting that P7C3 induced normal physiologic fiber maturation (Fig. 3B, C). In addition, the thickness of myelinated fibers in P7C3-treated rats was the same as that of naïve animals (Fig. 3D). Lower doses of

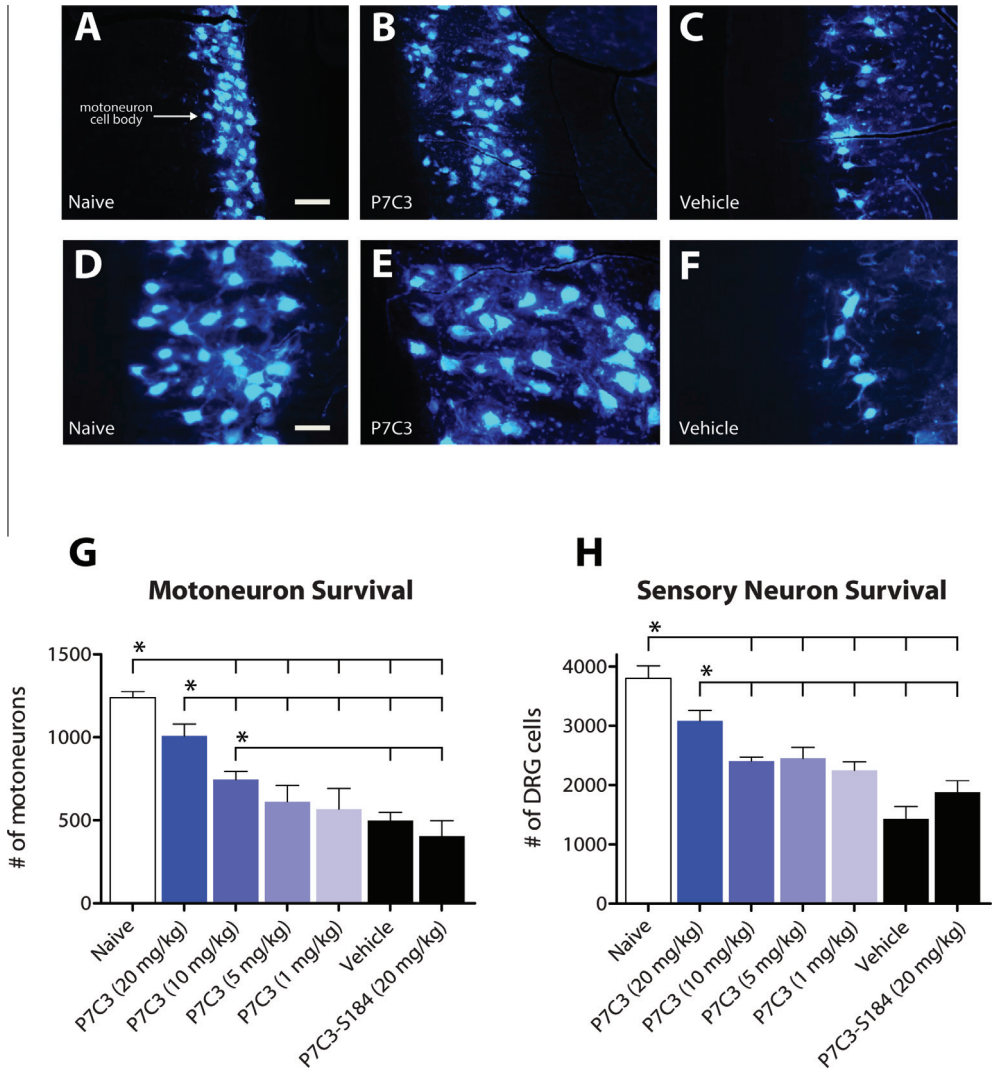

Fig. 2. P7C3 protects motor and sensory neurons from death 1 month following nerve crush injury. Retrogradely labeled spinal motoneurons at both low and high magnification (10–20×) from naïve animals (A, D), P7C3 at 20 mg/kg/d (B, E), and vehicle controls (C, F. Scale bar: A–C = 250 μm; D–F = 20 μm) illustrate the protective efficacy of P7C3. (G) P7C3 enhanced motoneuron survival at 1 month post-injury at a dose of 20 mg/kg/d compared with vehicle controls. H. P7C3 enhanced dorsal root ganglion sensory neuron survival at a dose of 20 mg/kg/d. *Mean + SEM, $p < 0.01$.

P7C3 or vehicle treatment, however, were associated with abnormally thickened myelination in addition to lower numbers of regenerating axons (Fig. 3B), as assessed by the ratio of axonal diameter to total fiber diameter, known as the g-ratio, for which we observed a significant group effect [$F_{(6,23)} = 10.68$, $p < 0.01$]. Naïve rats, or rats receiving P7C3 at 20 mg/kg/d after injury, displayed higher g-ratios than rats receiving lower doses of P7C3 or vehicle, indicating that treatment with P7C3 restored normal myelination in addition to axonal outgrowth following protection of both DRG sensory neurons and ventral horn motoneurons (Fig. 3C).

P7C3 restored behavioral function following injury

Because gait development in rats is complete by P27 (Shriner et al., 2009), we assessed performance of three groups of rats (uninjured controls, P7C3 [20 mg/kg/d]-treated, and vehicle controls) in locomotor tasks five weeks after injury. Throughout these tasks, animal velocity was held constant and measured velocity was not different between groups, an important control as differences in animal velocity alter stance duration and stride length (Shenaq et al., 1989; Varejao et al., 2004; Boyd et al., 2007). Locomotor recovery was first assessed with the SFI, which generates scores that range from 0 (uninjured) to -100 (completely impaired sciatic nerve function) as rats traverse a track at a standard velocity of 60 to 90 cm/s (Muir and Webb, 2000; Webb and Muir, 2004). Testing began five weeks after sciatic nerve crush injury and was conducted weekly for the following eight weeks. As expected, naïve rats maintained normal SFI values throughout the entire 8-week testing period (Fig. 4A). However, vehicle control SFI values five weeks after injury plateaued at a mean SFI of -45, indicating poor behavioral recovery. Although SFI among the P7C3-treated rats was initially poor, by week eight the P7C3-treated rats exhibited improved SFI scores to levels

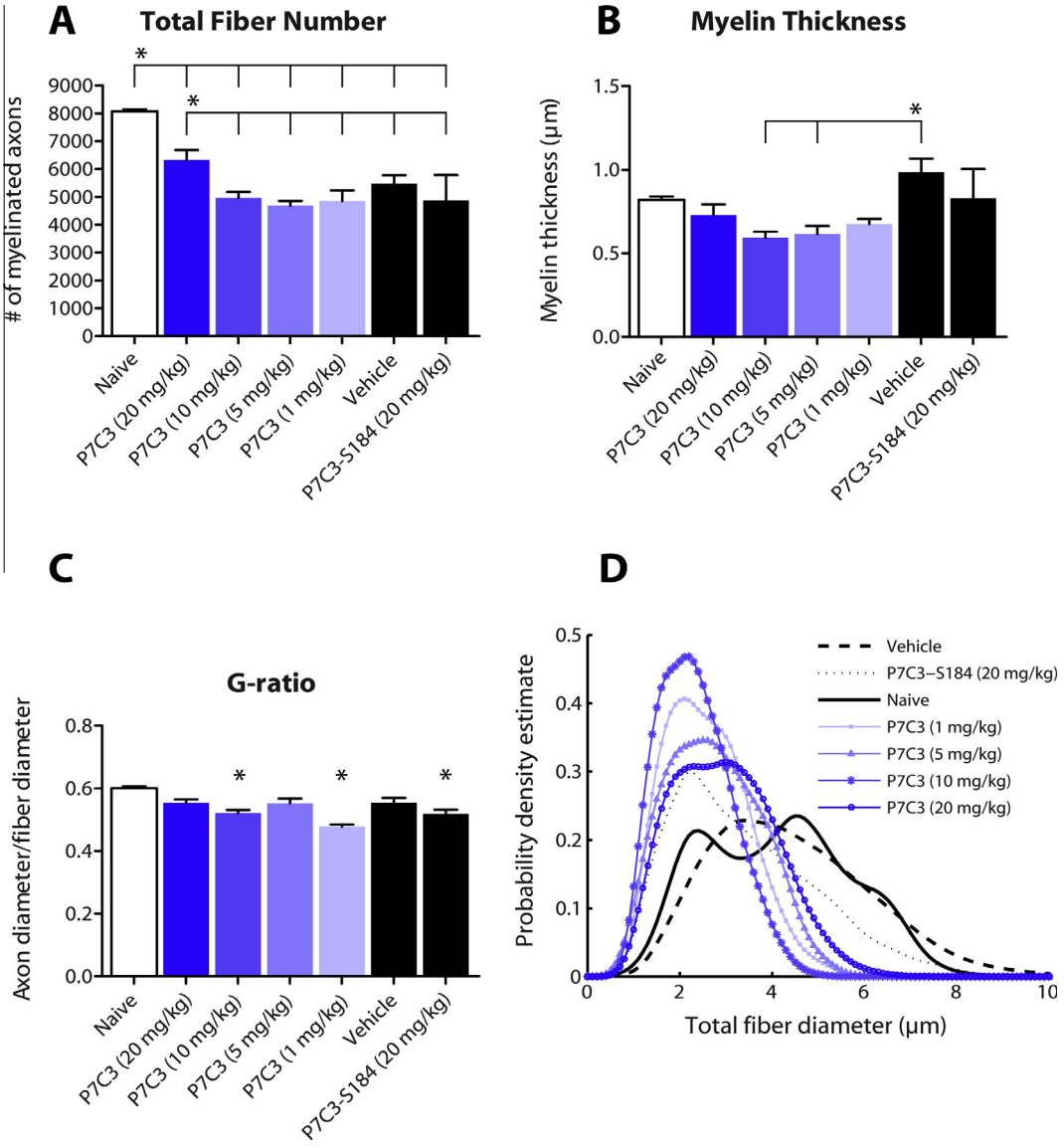

Fig. 3. P7C3 enhances axonal regeneration following neonatal nerve injury. (A) Naïve animals displayed a statistically greater number of total myelinated fibers than all other groups. Rats receiving P7C3 at a dose of 20 mg/kg/d regenerated more myelinated fibers than did rats receiving vehicle or lower doses of P7C3 after injury. (B) Normal thickness of myelin was preserved in P7C3-treated animals at the highest dose of P7C3 tested, whereas rats treated with lower doses of P7C3 or with vehicle developed abnormally thick myelin in regenerating axons. (C) Rats receiving P7C3 (1 or 10 mg/kg), vehicle, or the inactive analog P7C3-S184 had statistically lower g-ratios after injury than naive animals or injured animals that received 20 mg/kg/d P7C3, consistent with the observation that efficacious doses of P7C3 preserve normal myelin thickness in regenerating axons. (D) Density plot of the total number of myelinated fiber distribution shows that rats receiving P7C3 (20 mg/kg/d) display a similar distribution profile to that of naïve animals. *Mean + SEM, $p < 0.05$.

equivalent to those of the naïve rats [$F_{(6,17)} = 4.71$, $p < 0.01$; Fig. 4A].

We also evaluated the effect of P7C3 on skilled locomotion with the more challenging ledged tapered beam test. In this task, rats are trained to traverse an elevated beam that is tapered along its length and has an underhanging ledge that the rat can use as a crutch if it slips (Zhao et al., 2005). Footfaults (slips) are measured as an index of hindlimb function, calculated as the hindlimb slip ratio (number of right hindlimb slips per total right hindlimb steps x 100). Consistent with previous research, all rats ambulated across the tapered beam at a constant velocity (Kemp et al., 2011, 2013), and naive rats generated a slip ratio under 10% throughout the testing period. Injured rats, however, generated a slip ratio around 30% (Fig. 4B). Notably, injured rats that were treated with P7C3 showed 20% improved slip ratios by seven weeks following injury, and outperformed vehicle control rats for the remainder of the study [$F_{(6,17)} = 14.09$, $p < 0.01$; Fig. 4B].

We also assessed skilled locomotion using the ladder rung rest, which requires the rat to serially aim for the appropriate rung, accurately place its paw, and then grasp the rung (Metz and Whishaw, 2002; Kemp et al., 2011). Because rung spacing is varied between trials, this test controls for the rat's ability to learn the task. Naive

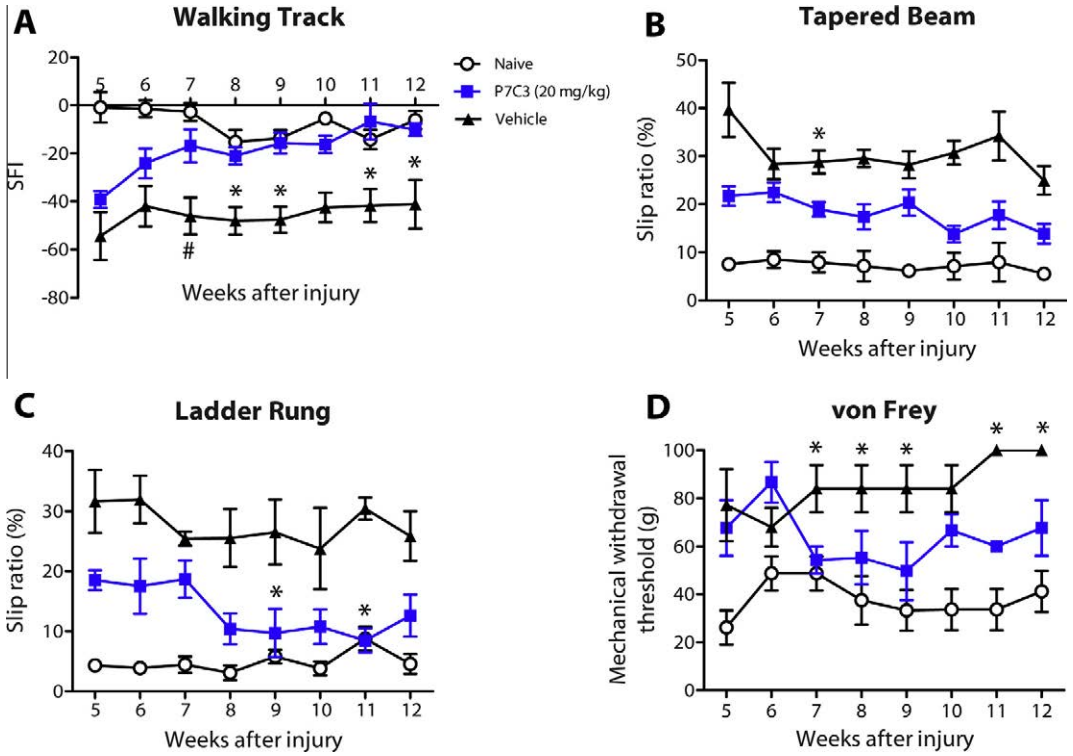

Fig. 4. P7C3 enhances behavioral recovery following neonatal nerve injury. (A) Rats receiving P7C3 improved their sciatic functional index on the walking track in overground locomotor analysis. Their scores improved over time, and surpassed scores in the vehicle-treated group by 5 weeks after injury ($^{\#}p < 0.01$). P7C3-treated rats recovered to naive control values, with SFIs equivalent to normal controls by eight weeks after injury ($^{*}p < 0.01$). B. A slip ratio was calculated in the tapered beam assay of skilled locomotion as the number of right hindlimb slips per total number of right hindlimb steps × 100%. Injured rats receiving P7C3 generated lower slip ratios than vehicle control injured animals from week eight onward ($^{*}p < 0.01$). C. In the ladder rung test of skilled locomotion, rats receiving P7C3 showed improved slip ratios compared with vehicle-treated rats at all weeks tested, and their slip ratios were equivalent to those of naive rats by week ten ($^{*}p < 0.01$). (D) The von Frey test, in which the paw was stimulated with monofilaments, demonstrated that treatment with P7C3 improved recovery of cutaneous sensation compared with the vehicle controls ($^{*}p < 0.01$).

and P7C3-treated rats yielded significantly better slip ratios than vehicle control rats at all time points [$F_{(6,17)} = 9.98$, $p < 0.01$], and P7C3-treated rats developed slip ratios statistically equivalent to those of naïve animals by nine weeks following injury (Fig. 4C).

In addition to motor recovery, sensory function is also a high priority in patient recovery, as patients with insensate limbs are prone to self-injury from burns and trauma in early childhood (Borschel and Clarke, 2009). We thus assessed cutaneous sensation by measuring the withdrawal latency of the animal's affected right hindlimb using the von Frey test (Kemp et al., 2011). Vehicle control rats were less sensitive than either naive rats or P7C3-treated rats beginning at test week 7 and throughout the remainder of the testing period. P7C3-treated rats showed improved sensory recovery to a level intermediate between that of the vehicle and uninjured control groups [$F_{(6,17)} = 4.71$, $p < 0.01$; Fig. 4D].

P7C3 enhanced muscle force, muscle reinnervation, and muscle mass

In order to determine the effect of P7C3 on muscle force, we performed *in vivo* muscle force testing on the rats that underwent behavioral testing twelve weeks after injury. Specifically, we measured the isometric twitch and tetanic contractile force produced by the EDL muscle upon electrical stimulation of the sciatic nerve. P7C3-treated rats developed greater twitch muscle force compared to vehicle control rats [$F_{(2,16)} = 20.70$, $p < 0.01$; Fig. 5A]. P7C3-treated rats also developed greater tetanic muscle force compared to vehicle control rats, and their muscle forces were statistically equivalent to those of naïve rats [$F_{(2,16)} = 10.12$, $p < 0.01$; Fig. 5B].

In order to determine whether the improvement in muscle force in P7C3-treated rats was associated with an increase in motor nerve fibers re-innervating the EDL muscle, we recorded the twitch force following suprathreshold (2×) stimulation of the sciatic nerve. We then recorded all-or-none increments in twitch force in response to gradual increases in stimulus voltage from zero. We estimated the number of motor axons reinnervating the EDL muscle (motor unit number estimation, or MUNE) by calculating the ratio of the maximal muscle twitch force and the mean motor unit twitch force (McComas et al., 1971). The MUNE in naive rats was greater than that of the vehicle group, and the MUNE in P7C3-treated rats was equivalent to that of uninjured rats [$F_{(2,16)} = 2.48$, $p < 0.05$; Fig. 5C]. Thus, P7C3 treatment promoted nerve regeneration and reinnervation of EDL muscles to levels statistically equivalent to that of naive rats.

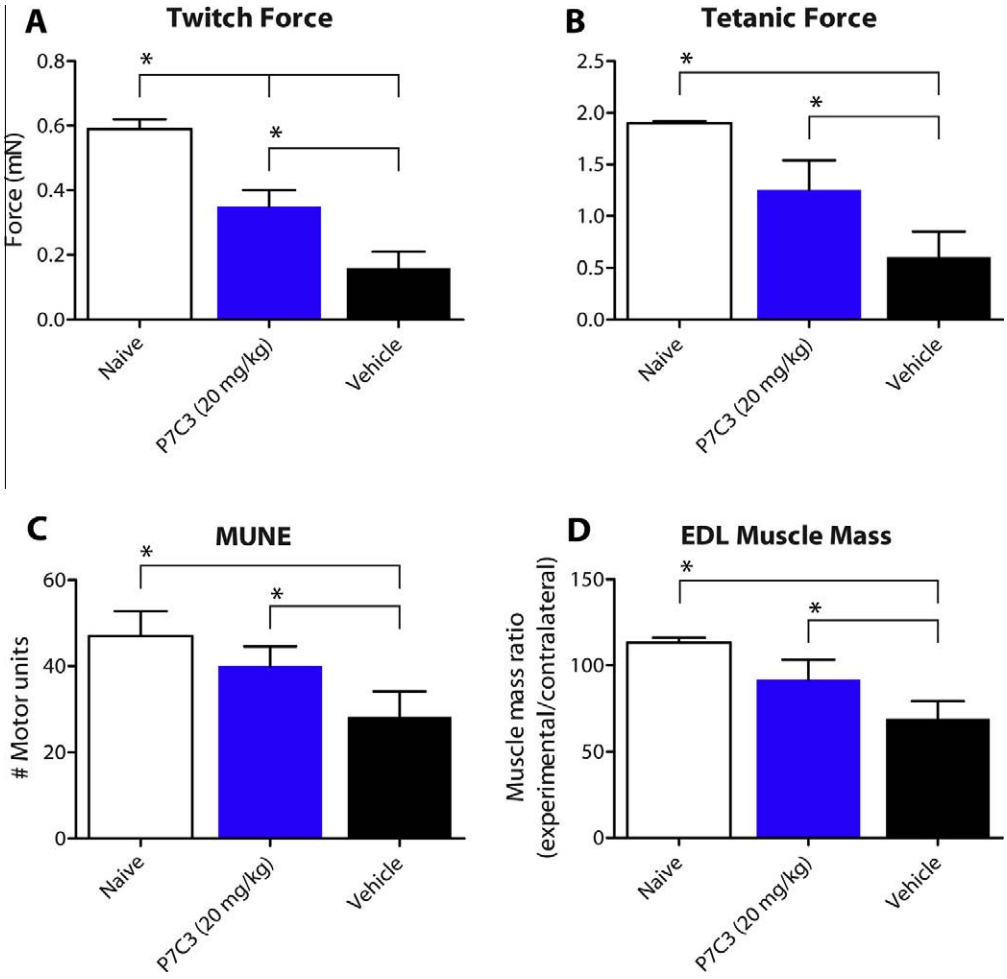

Fig. 5. P7C3 enhances recovery of muscle force, the total number of motor units, and muscle mass following neonatal nerve injury. Functional recovery after sciatic nerve crush injury was assessed by measuring the isometric twitch and tetanic force produced by the extensor digitorum longus (EDL) muscle in response to stimulation of the sciatic nerve, the total number of motor units (MUNE), and the wet muscle mass of the EDL muscle. (A) Rats receiving P7C3 generated higher mean twitch forces than did vehicle controls (*$p < 0.01$). (B) Uninjured control and P7C3-treated rat EDL muscles generated greater mean tetanic forces than did vehicle EDL muscles (*$p < 0.01$). (C) Naïve animals displayed a statistically greater number of motor units than vehicle controls, and did not differ from P7C3-treated rats (*$p < 0.05$). (D) Both naïve rats and P7C3-treated rats recovered more wet EDL muscle mass than did vehicle-treated rats, and did not differ from one another (*$p < 0.05$).

Next, we measured wet muscle mass as an additional measure of skeletal muscle recovery after nerve injury and reinnervation. Wet muscle mass correlates with muscle reinnervation, because this reverses denervation-associated atrophy (Katayama et al., 2006; Wood et al., 2011). After completing behavioral testing and muscle force recordings, we removed and weighed the EDL muscle from the injured and contralateral hindlimbs and calculated the muscle mass ratio (experimental side/contralateral side). EDL muscle masses from both naive and P7C3-treated rats were greater than vehicle controls, and did not differ significantly from one another [$F_{(2,16)} = 6.86$, $p < 0.05$; Fig. 5D]. Taken together, P7C3 treatment after injury enhanced recovery of muscle force, reinnervation and muscle mass.

P7C3 neuronal protection is not mediated through ionotropic glutamate receptors

Because ionotropic glutamate receptors have been previously implicated as therapeutic targets for protection of peripheral nerves from cell death following injury, (Cabaj and Slawinska, 2012; Petsanis et al., 2012), we investigated whether P7C3 might act on these receptors. K_i determination from ligand displacement studies at the three ionotropic glutamate receptors (NMDA, AMPA, and kainate), however, showed no activity of P7C3 at any receptor subtype (Fig. 6A–C).

P7C3 prevents microglia proliferation following nerve crush injury. Microglia, which are the resident macrophages and only immune cells in the CNS (Kreutzberg, 1996), proliferate in the spinal cord after peripheral nerve injury and adopt an activated state capable of inducing a highly neurotoxic environment (Beggs and Salter, 2007; Block et al., 2007). Specifically, activated microglia produce and secrete pro-inflammatory cytokines and neurotoxic molecules, and exhibit characteristic ameboid morphology (Gonzalez-Scarano and Baltuch, 1999; Tolosa et al., 2011). In order to determine whether the protective effect of P7C3 was associated with

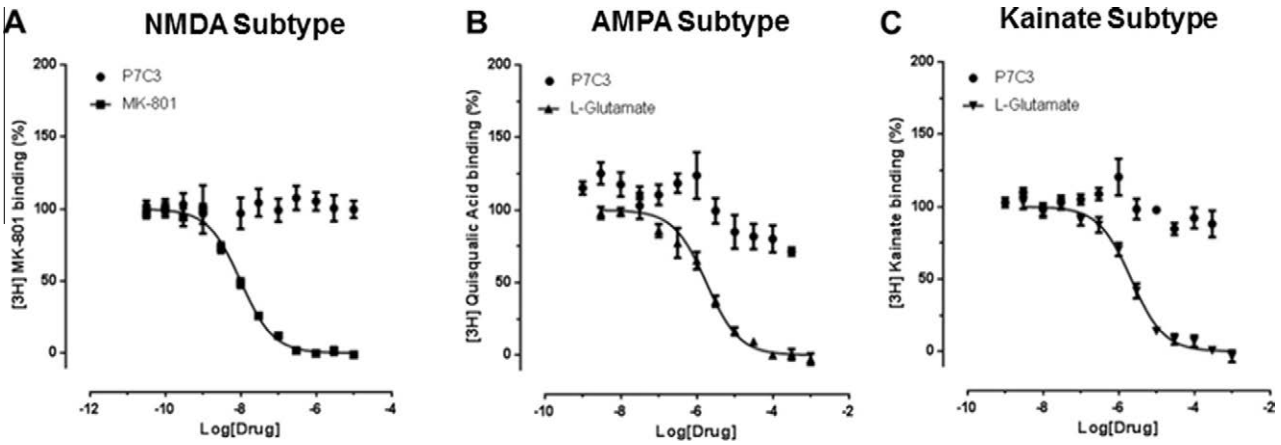

Fig. 6. Glutamate receptors are not the target of P7C3-mediated neuronal protection. Ligand displacement studies with P7C3 at ionotropic glutamate receptors demonstrate that the neuroprotective efficacy of P7C3 is not attributed to activity at either (A) the NMDA subtype; (B) the AMPA subtype, or; (C) the kainate receptor subtype.

mitigation of microglia activation, we performed immunohistochemical analysis of microglia on spinal cord sections one month following initial injury and treatment. Fig. 7A shows a stereotypical transverse spinal cord slice, with the four areas investigated in white boxes (ipsi and contralateral dorsal and ventral horns). We found a significant group effect for the ipsilateral dorsal horn [$F_{(2,14)}$ = 16.20, p < .001], whereby microglia numbers were significantly higher in the crush group treated with vehicle than either the naïve or crush group treated with P7C3. Both naïve animals and those treated with P7C3 did not differ statistically from one another (Fig. 7B). In addition to limited microglia proliferation, animals administered P7C3 also showed a decrease in the characteristic ameboid morphology, which was highly prevalent in vehicle-treated animals. We found a similar effect for the ipsilateral ventral horn [$F_{(2,14)}$ = 15.45, p < .001], in which crush-injured animals administered vehicle displayed significantly higher microglia numbers, while P7C3 treated and naïve animals did not differ from one another (Fig. 7B). We also found a surprising contralateral effect in the ventral horn [F(2,14) = 7.40, p < .05]. Here, crush-injured animals administered vehicle displayed significantly higher microglia numbers than naïve animals. Taken together, these results suggest that administration of P7C3 stabilized microglia numbers following nerve crush injury, suggesting that the health of the neurons was greater following P7C3 administration.

DISCUSSION

We have demonstrated potent neuroprotective efficacy of P7C3 in a preclinical model of traumatic peripheral nerve injury, a devastating form of neonatal neurological injury that currently lacks any pharmacologic treatment options. P7C3 doubled peripheral neuron survival, preserving 80% of both motor and sensory neurons when administered daily for two weeks following injury on postnatal day 3. Treatment with P7C3 also enhanced axonal regeneration and restored normal myelin thickness after injury in peripheral neurons, akin to what has been reported on efficacy of P7C3 compounds on blocking axonal degeneration in the brain (Yin et al., 2014). P7C3 also greatly enhanced sensorimotor function, one of the most important considerations for patients affected by nerve injuries (Winfree, 2005; Dolan et al., 2012). Specifically, injured rats treated with P7C3 showed significantly improved performance in multiple tasks of locomotion, approaching or equaling performance levels of naive rats. Previous research has consistently shown a lack of pain behaviors following both sciatic and dorsal root lesions, since the capacity to evoke behavioral responses is limited when sensory reinnervation is poor (Sheen and Chung, 1993; Yoon et al., 1996), as was the case with the vehicle group in our study. P7C3-treated rats, however, recovered footpad sensation more rapidly than vehicle-treated controls, correlating with the increased number of surviving DRG sensory neurons. P7C3 treatment also improved contractile force and muscle mass 12 weeks after sciatic nerve crush injury to levels approximating those of naïve animals. Finally, treatment with P7C3 prevented proliferation of microglia cells following injury, returning the regenerative microenvironment to a level indistinguishable from naïve animals. We are not aware of any other pharmacologic treatments, including glutamate receptor antagonists and neurotrophic factors, that have demonstrated equivalent neuroprotective efficacy following neonatal peripheral nerve injury (Mentis et al., 1993; Aszmann et al., 2002, 2004; Kapoukranidou et al., 2005; Gougoulias et al., 2007; Cabaj and Slawinska, 2012).

Microglia, the resident immune cells of the CNS, are upregulated by both motor and sensory neuronal death following neonatal nerve injury (Morioka and Streit, 1991). Once activated, microglia proliferate rapidly and secrete pro-inflammatory cytokines, chemokines, and neurotoxic molecules that contribute to a toxic microenvironment leading to neuronal death (Beggs and Salter, 2007; Block et al., 2007; Benarroch, 2013). P7C3 has been shown to foster stabilization of mitochondrial membrane potential in the face of otherwise overwhelming toxic insult (Pieper et al., 2010),and P7C3 may be acting directly on neurons in our model. In our model, neuronal

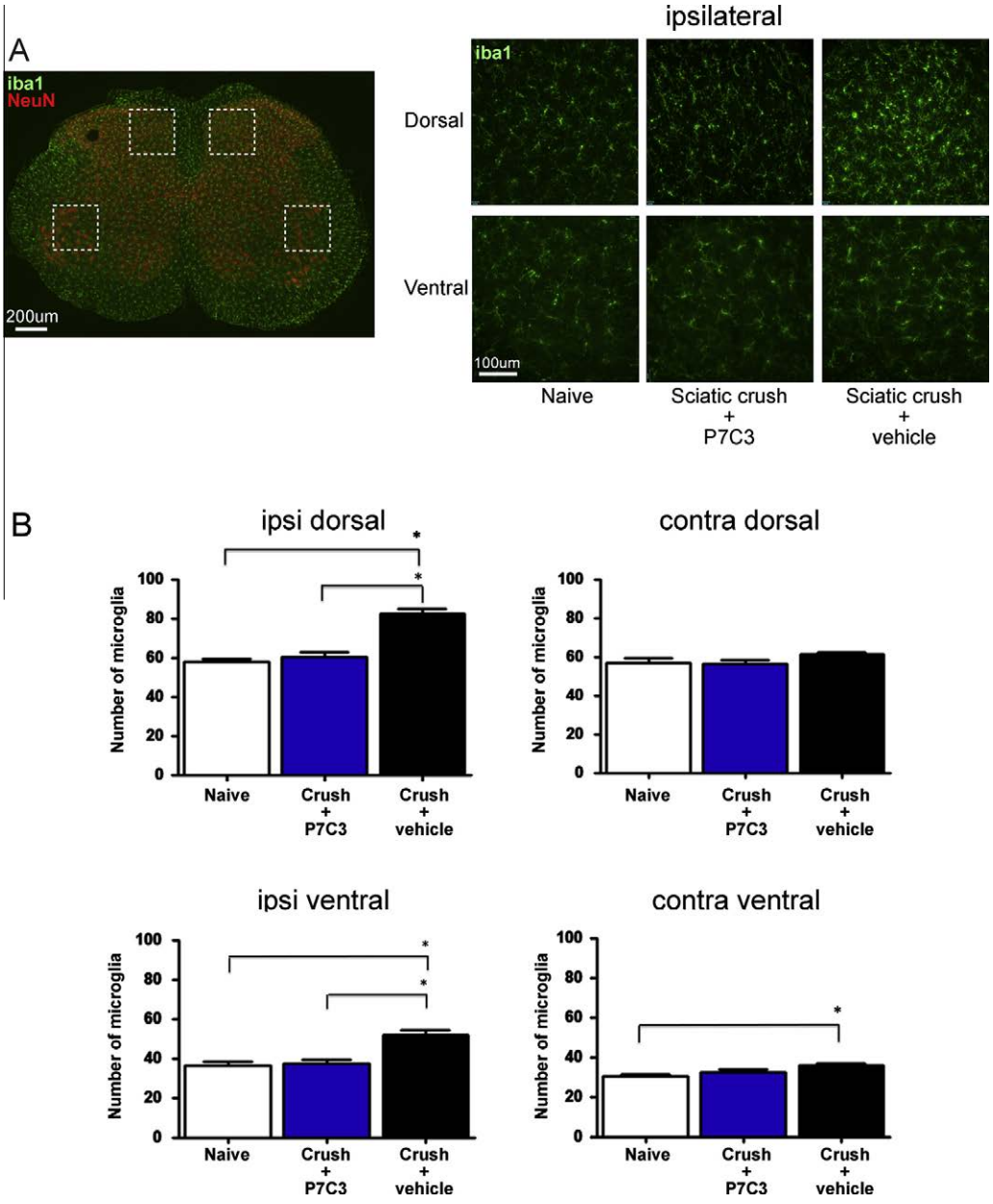

Fig. 7. P7C3 restores the microglia milieu in the ventral and dorsal horns of the spinal cord. (A) Right: Representative transverse section of the spinal cord of a naïve animal, with neurons stained with NeuN (red), and microglia stained with Iba-1 (green). Left: Representative sections of ipsilateral dorsal and ventral horns of the spinal cord in naïve, P7C3-treated, and vehicle-treated animals following crush injury. (B) Crush-injured animals treated with vehicle displayed significantly greater microglia numbers than either naïve or P7C3-treated animals in both the ipsilateral dorsal and ventral horns. P7C3-treated and naïve animals did not differ statistically from one another in either ipsilateral horn. Interestingly, vehicle-treated animals following crush injury displayed significantly greater microglia numbers than naïve animals in the contralateral ventral horn, while P7C3-treated and naïve animals did not differ from one another. The reduction in microgliosis suggests that P7C3 improves overall neuron health in the dorsal and ventral horns. (For interpretation of the references to color in this figure legend, the reader is referred to the web version of this article.)

rescue could also be related to a reduced toxic effect of activated microglia mediated by P7C3. For example, neuroprotection against cell death could decrease pathologic signaling to microglia and thus foster a less toxic environment, and contribute to the lack of observed increased stereotypical microgliosis around dead and/or dying neurons following P7C3.

There are no pharmacologic treatment options to augment treatment of newborn children with peripheral nerve injuries. Currently, recovery depends exclusively on surgery and rehabilitative physiotherapy, which are often insufficient (Borschel and Clarke, 2009). Because the potential for successful functional recovery from neonatal nerve injury increases as the number of available neurons increases (Fu and Gordon, 1995a; Fu and Gordon, 1995b), rescuing neurons with systemic administration of a neuroprotective agent like P7C3 could enhance re-innervation of target end organs and improve patient outcomes. A pharmacological approach to treating peripheral nerve injury would revolutionize treatment of this common debilitating condition by allowing clinicians to initiate immediate treatment.

Currently, nerve injuries in newborns and adults are unable to be effectively addressed as medical emergencies. Rather, clinicians generally wait three months to see whether the nerve recovers on its own. If it does not, then they operate on the injured part of the nerve. Unfortunately, by three months most of the potential for axon regeneration has deteriorated because both the neuron's cell body and its associated Schwann cells lose their capacity for regeneration over time. An agent that could rescue neurons after nerve injury would thus allow clinicians to advance the management of nerve injuries from the current three month ''wait-and-see'' approach to one of active neuron rescue. By saving more neurons, an injured nerve's recovery could be enhanced and, in turn, patients may recover faster and more completely, reducing and in some cases even eliminating the need for surgery. Importantly, the P7C3-series of neuroprotective agents have a large therapeutic window and lack any known toxicity. Therefore we believe that this family of compounds represents a practical basis for developing a pharmacologic treatment option for patients with nerve injury.

Acknowledgments and financial disclosure—The authors are grateful to Jennifer Zhang and Cameron Chiang for expert technical assistance, Dr. Graham Pitcher for the use of the von Frey apparatus, and to Amy Tan for help with immunohistochemical protocols. This research was supported by grants from the Canadian Institute of Health Research (CIHR), the National Institute of Health (NIH), the Plastic Surgery Foundation (PSF), and National Institutes of Mental Health (NIMH) 1R01MH087986 to A.A.P. and Steven L. McKnight. At no time did any funding source have an involvement in either the design of the research, preparation of the manuscript, or the decision to submit the manuscript to a scientific journal. Dr. Kemp was supported through postdoctoral fellowship grants from the IAMGOLD Corporation and the Hospital for Sick Children RESTRACOMP program. The authors thank the National Institute of Mental Health's Psychoactive Drug Screening Program for K_i determinations of receptor binding (contract # HHSN-271-2008-00025-C (NIMH PDSP), directed by Bryan L. Roth MD, PhD at the University of North Carolina at Chapel Hill and Project Officer Jamie Driscol at NIMH, Bethesda MD, USA.

REFERENCES

Abercrombie M (1946) Estimation of nuclear population from microtome sections. Anat Rec 94:239–247.

Akel BS, Oksuz C, Oskay D, Firat T, Tarakci E, Leblebicioglu G (2013) Health-related quality of life in children with obstetrical brachial plexus palsy. Qual Life Res.

Alant JD, Kemp SW, Khu KJ, Kumar R, Webb AA, Midha R (2011) Traumatic neuroma in continuity injury model in rodents. J Neurotrauma.

Asai-Coakwell M, March L, Dai XH, Duval M, Lopez I, French CR, Famulski J, De BE, Francis PJ, Sundaresan P, Sauve Y, Koenekoop RK, Berry FB, Allison WT, Waskiewicz AJ, Lehmann OJ (2013) Contribution of growth differentiation factor 6-dependent cell survival to early-onset retinal dystrophies. Hum Mol Genet 22:1432–1442.

Aszmann OC, Korak KJ, Kropf N, Fine E, Aebischer P, Frey M (2002) Simultaneous GDNF and BDNF application leads to increased motoneuron survival and improved functional outcome in an experimental model for obstetric brachial plexus lesions. Plast Reconstr Surg 110:1066–1072.

Aszmann OC, Winkler T, Korak K, Lassmann H, Frey M (2004) The influence of GDNF on the time course and extent of motoneuron loss in the cervical spinal cord after brachial plexus injury in the neonate. Neurol Res 26:211–217.

Bahadori MH, Al-Tiraihi T, Valojerdi MR (2001) Sciatic nerve transection in neonatal rats induces apoptotic neuronal death in L5 dorsal root ganglion. J Neurocytol 30:125–130.

Bain JR, Mackinnon SE, Hunter DA (1989) Functional evaluation of complete sciatic, peroneal, and posterior tibial nerve lesions in the rat. Plast Reconstr Surg 83:129–138.

Barr JS, Katz KA, Hazen A (2011) Surgical management of facial nerve paralysis in the pediatric population. J Pediatr Surg 46: 2168–2176.

Beggs S, Salter MW (2007) Stereological and somatotopic analysis of the spinal microglial response to peripheral nerve injury. Brain Behav Immun 21:624–633.

Benarroch EE (2013) Microglia: multiple roles in surveillance, circuit shaping, and response to injury. Neurology 81: 1079–1088.

Blaya MO, Bramlett HM, Naidoo J, Pieper AA, Dietrich WD (2013) Neuroprotective efficacy of a proneurogenic compound after traumatic brain injury. J Neurotrauma.

Blaya MO, Bramlett HM, Naidoo J, Pieper AA, Dietrich WD (2014) Neuroprotective efficacy of a proneurogenic compound after traumatic brain injury. J Neurotrauma 31:476–486.

Block ML, Zecca L, Hong JS (2007) Microglia-mediated neurotoxicity: uncovering the molecular mechanisms. Nat Rev Neurosci 8: 57–69.

Borschel GH, Clarke HM (2009) Obstetrical brachial plexus palsy. Plast Reconstr Surg 124:144e–155e.

Boyd BS, Puttlitz C, Noble-Haeusslein LJ, John CM, Trivedi A, Topp KS (2007) Deviations in gait pattern in experimental models of hindlimb paresis shown by a novel pressure mapping system. J Neurosci Res 85:2272–2283.

Bridge PM, Ball DJ, Mackinnon SE, Nakao Y, Brandt K, Hunter DA, Hertl C (1994) Nerve crush injuries–a model for axonotmesis. Exp Neurol 127:284–290.

Buitenhuis S, van Wijlen-Hempel RS, Pondaag W, Malessy MJ (2012) Obstetric brachial plexus lesions and central developmental disability. Early Hum Dev 88:731–734.

Cabaj AM, Slawinska U (2012) Riluzole treatment reduces motoneuron death induced by axotomy in newborn rats. J Neurotrauma 29:1506–1517.

Choi DW (1988) Glutamate neurotoxicity and diseases of the nervous system. Neuron 1:623–634.

De Jesus-Cortes H, Xu P, Drawbridge J, Estill SJ, Huntington P, Tran S, Britt J, Tesla R, Morlock L, Naidoo J, Melito LM, Wang G, Williams NS, Ready JM, McKnight SL, Pieper AA (2012) Neuroprotective efficacy of aminopropyl carbazoles in a mouse model of Parkinson disease. Proc Natl Acad Sci U S A 109:17010–17015.

de Medinaceli L, Freed WJ, Wyatt RJ (1982) An index of the functional condition of rat sciatic nerve based on measurements made from walking tracks. Exp Neurol 77:634–643.

Dekkers J, Waters J, Vrbová G, Greensmith L (2001) Treatment of the neuromuscular junction with 4-aminopyridine results in improved reinnervation following nerve injury in neonatal rats. Neuroscience 103:267–274.

Dolan RT, Butler JS, Murphy SM, Hynes D, Cronin KJ (2012) Health-related quality of life and functional outcomes following nerve transfers for traumatic upper brachial plexus injuries. J Hand Surg Eur 37:642–651.

Dutca LM, Stasheff SF, Heberg-Buenz A, Rudd D, Batra N, Blodi FR, Yorek M, Yin T, Shankar M, Herlein J, Naidoo J, Morlock L, Williams NS, Kardon RH, Anderson MG, Pieper AA, Harper MM (2014) Early and noninvasive detection of subclinical visual damage after blast-mediated traumatic brain injury enables prevention of chronic visual deficit by treatment with P7C3-S243. Neuroscience.

Fattah A, Borschel GH, Zuker RM (2011) Reconstruction of facial nerve injuries in children. J Craniofac Surg 22:782–788.

Firat T, Oskay D, Akel BS, Oksuz C (2012) Impact of obstetrical brachial plexus injury on parents. Pediatr Int 54:881–884.
Fu SY, Gordon T (1995a) Contributing factors to poor functional recovery after delayed nerve repair: prolonged axotomy. J Neurosci 15:3876–3885.
Fu SY, Gordon T (1995b) Contributing factors to poor functional recovery after delayed nerve repair: prolonged denervation. J Neurosci 15:3886–3895.
Gonzalez-Scarano F, Baltuch G (1999) Microglia as mediators of inflammatory and degenerative diseases. Annu Rev Neurosci 22:219–240.
Gougoulias N, Kouvelas D, Albani M (2007) Protective effect of PNQX on motor units and muscle property after sciatic nerve crush in neonatal rats. Pharmacol Res 55:370–377.
Hasegawa S, Kohro Y, Shiratori M, Ishii S, Shimizu T, Tsuda M, Inoue K (2010) Role of PAF receptor in proinflammatory cytokine expression in the dorsal root ganglion and tactile allodynia in a rodent model of neuropathic pain. PLoS One 5:e10467.
Hegedus J, Putman CT, Gordon T (2007) Time course of preferential motor unit loss in the SOD1(G93A) mouse model of amyotrophic lateral sclerosis. Neurobiol Dis 28:154–164.
Jenq CB, Coggeshall RE (1985) Numbers of regenerated axons in tributary nerves following neonatal sciatic nerve crush in rat. Neurosci Lett 61:43–48.
Kalmar B, Burnstock G, Vrbová G, Urbanics R, Csermely P, Greensmith L (2002) Upregulation of heat shock proteins rescues motoneurones from axotomy-induced cell death in neonatal rats. Exp Neurol 176:87–97.
Kapoukranidou D, Gougoulias N, Hatzisotiriou A, Fardi D, Albani M, Kalpidis I (2005) Assessment of motoneuron death during development following neonatal nerve crush and Mg2+ treatment. Med Sci Monit 11:BR373–BR379.
Katayama Y, Montenegro R, Freier T, Midha R, Belkas JS, Shoichet MS (2006) Coil-reinforced hydrogel tubes promote nerve regeneration equivalent to that of nerve autografts. Biomaterials 27:505–518.
Kemp SW, Alant J, Walsh SK, Webb AA, Midha R (2010) Behavioural and anatomical analysis of selective tibial nerve branch transfer to the deep peroneal nerve in the rat. Eur J Neurosci 31:1074–1090.
Kemp SW, Phua PD, Stanoulis KN, Wood MD, Liu EH, Gordon T, Borschel GH (2013) Functional recovery following peripheral nerve injury in the transgenic Thy1-GFP rat. J Peripher Nerv Syst 18:220–231.
Kemp SW, Webb AA, Dhaliwal S, Syed S, Walsh SK, Midha R (2011) Dose and duration of nerve growth factor (NGF) administration determine the extent of behavioral recovery following peripheral nerve injury in the rat. Exp Neurol 229:460–470.
Kemp SWP, Syed S, Walsh W, Zochodne DW, Midha R (2009) Collagen nerve conduits promote enhanced axonal regeneration, Schwann cell association, and neovascularization compared to silicone conduits. Tissue Eng Part A 15:1975–1988.
Kozin SH (2011) The evaluation and treatment of children with brachial plexus birth palsy. J Hand Surg Am 36:1360–1369.
Kreutzberg GW (1996) Microglia: a sensor for pathological events in the CNS. Trends Neurosci 19:312–318.
Lapper SR, Brown MC, Perry VH (1994) Motor neuron death induced by axotomy in neonatal mice occurs more slowly in a mutant strain in which Wallerian degeneration is very slow. Eur J Neurosci 6:473–477.
Lawson SJ, Lowrie MB (1998) The role of apoptosis and excitotoxicity in the death of spinal motoneurons and interneurons after neonatal nerve injury. Neuroscience 87:337–348.
Lewis SE, Mannion RJ, White FA, Coggeshall RE, Beggs S, Costigan M, Martin JL, Dillmann WH, Woolf CJ (1999) A role for HSP27 in sensory neuron survival. J Neurosci 19:8945–8953.
Lowrie MB, Krishnan S, Vrbová G (1987) Permanent changes in muscle and motoneurones induced by nerve injury during a critical period of development of the rat. Brain Res 428:91–101.
Lowrie MB, Lavalette D, Davies CE (1994) Time course of motoneurone death after neonatal sciatic nerve crush in the rat. Dev Neurosci 16:279–284.
Lowrie MB, Vrbova G (1984) Different pattern of recovery of fast and slow muscles following nerve injury in the rat. J Physiol 349:397–410.
MacMillan KS, Naidoo J, Liang J, Melito L, Williams NS, Morlock L, Huntington PJ, Estill SJ, Longgood J, Becker GL, McKnight SL, Pieper AA, De Brabander JK, Ready JM (2011) Development of proneurogenic, neuroprotective small molecules. J Am Chem Soc 133:1428–1437.
Major LA, Hegedus J, Weber DJ, Gordon T, Jones KE (2007) Method for counting motor units in mice and validation using a mathematical model. J Neurophysiol 97:1846–1856.
Major LA, Jones KE (2005) Simulations of motor unit number estimation techniques. J Neural Eng 2:17–34.
Malessy MJ, Pondaag W (2009) Obstetric brachial plexus injuries. Neurosurg Clin N Am 20:1–14. v.
Malessy MJ, Pondaag W (2011) Nerve surgery for neonatal brachial plexus palsy. J Pediatr Rehabil Med 4:141–148.
McComas AJ, Fawcett PR, Campbell MJ, Sica RE (1971) Electrophysiological estimation of the number of motor units within a human muscle. J Neurol Neurosurg Psychiatry 34:121–131.
Mehta A, Prabhakar M, Kumar P, Deshmukh R, Sharma PL (2013) Excitotoxicity: bridge to various triggers in neurodegenerative disorders. Eur J Pharmacol 698:6–18.
Mentis GZ, Greensmith L, Vrbova G (1993) Motoneurons destined to die are rescued by blocking N-methyl-D-aspartate receptors by MK-801. Neuroscience 54:283–285.
Metz GA, Whishaw IQ (2002) Cortical and subcortical lesions impair skilled walking in the ladder rung walking test: a new task to evaluate fore- and hindlimb stepping, placing, and co-ordination. J Neurosci Methods 115:169–179.
Monte-Raso VV, Barbieri CH, Mazzer N, Yamasita AC, Barbieri G (2008) Is the sciatic functional index always reliable and reproducible? J Neurosci Methods 170:255–261.
More HL, Chen J, Gibson E, Donelan JM, Beg MF (2011) A semi-automated method for identifying and measuring myelinated nerve fibers in scanning electron microscope images. J Neurosci Methods 201:149–158.
Morioka T, Streit WJ (1991) Expression of immunomolecules on microglial cells following neonatal sciatic nerve axotomy. J Neuroimmunol 35:21–30.
Muir GD, Webb AA (2000) Mini-review: assessment of behavioural recovery following spinal cord injury in rats. Eur J Neurosci 12:3079–3086.
Naidoo J, Bember CJ, Allwein SR, Liang J, Pieper AA, Ready JM (2013) Development of a scalable synthesis of P7C3-A20, a potent neuroprotective agent. Tetrahedron Lett 54: 4429–4431.
Naidoo J, De Jesus-Cortes H, Huntington P, Estill S, Morlock LK, Starwalt R, Mangano TJ, Williams NS, Pieper AA, Ready JM (2014) Discovery of a neuroprotective chemical, (S)-N-(3-(3,6-dibromo-9H-carbazol-9-yl)-2-fluoropropyl)-6-methoxypyridin-2-amine [(-)-P7C3-S243], with improved drug like properties. J Med Chem 57:3746–3754.
Naumann T, Hartig W, Frotscher M (2000) Retrograde tracing with Fluoro-Gold: different methods of tracer detection at the ultrastructural level and neurodegenerative changes of back-filled neurons in long-term studies. J Neurosci Methods 103: 11–21.
Navarrete R, Vrbova G (1984) Differential effect of nerve injury at birth on the activity pattern of reinnervated slow and fast muscles of the rat. J Physiol 351:675–685.
Petsanis K, Chatzisotiriou A, Kapoukranidou D, Simeonidou C, Kouvelas D, Albani M (2012) Contractile properties and movement behaviour in neonatal rats with axotomy, treated with the NMDA antagonist DAP5. BMC Physiol 12:5.
Pham CB, Kratz JR, Jelin AC, Gelfand AA (2011) Child neurology: brachial plexus birth injury: what every neurologist needs to know. Neurology 77:695–697.
Phua PD, Al-Samkari HT, Borschel GH (2012) Is the term ‘‘obstetrical brachial plexus palsy’’ obsolete? An international survey to

assess consensus among peripheral nerve surgeons. J Plast Reconstr Aesthet Surg 65:1227–1232.
Pieper AA, McKnight SL, Ready JM (2014) P7C3 and an unbiased approach to drug discovery for neurodegenerative diseases. Chem Soc Rev 43:6716–6726.
Pieper AA, Xie S, Capota E, Estill SJ, Zhong J, Long JM, Becker GL, Huntington P, Goldman SE, Shen CH, Capota M, Britt JK, Kotti T, Ure K, Brat DJ, Williams NS, MacMillan KS, Naidoo J, Melito L, Hsieh J, De BJ, Ready JM, McKnight SL (2010) Discovery of a proneurogenic, neuroprotective chemical. Cell 142:39–51.
Pollin MM, McHanwell S, Slater CR (1991) The effect of age on motor neurone death following axotomy in the mouse. Development 112:83–89.
Pondaag W, Malessy MJ, van Dijk JG, Thomeer RT (2004) Natural history of obstetric brachial plexus palsy: a systematic review. Dev Med Child Neurol 46:138–144.
Raimondo S, Fornaro M, Di SF, Ronchi G, Giacobini-Robecchi MG, Geuna S (2009) Chapter 5: methods and protocols in peripheral nerve regeneration experimental research: part II-morphological techniques. Int Rev Neurobiol 87:81–103.
Sheen K, Chung JM (1993) Signs of neuropathic pain depend on signals from injured nerve fibers in a rat model. Brain Res 610:62–68.
Shenaq JM, Shenaq SM, Spira M (1989) Reliability of sciatic function index in assessing nerve regeneration across a 1 cm gap. Microsurgery 10:214–219.
Shriner AM, Drever FR, Metz GA (2009) The development of skilled walking in the rat. Behav Brain Res 205:426–435.
Squitieri L, Steggerda J, Yang LJ, Kim HM, Chung KC (2011) A national study to evaluate trends in the utilization of nerve reconstruction for treatment of neonatal brachial plexus palsy [outcomes article]. Plast Reconstr Surg 127:277–283.
Tesla R, Wolf HP, Xu P, Drawbridge J, Estill SJ, Huntington P, McDaniel L, Knobbe W, Burket A, Tran S, Starwalt R, Morlock L, Naidoo J, Williams NS, Ready JM, McKnight SL, Pieper AA (2012) Neuroprotective efficacy of aminopropyl carbazoles in a mouse model of amyotrophic lateral sclerosis. Proc Natl Acad Sci U S A 109:17016–17021.
Tolosa L, Caraballo-Miralles V, Olmos G, Llado J (2011) TNF-alpha potentiates glutamate-induced spinal cord motoneuron death via NF-kappaB. Mol Cell Neurosci 46:176–186.
Varejao AS, Melo-Pinto P, Meek MF, Filipe VM, Bulas-Cruz J (2004) Methods for the experimental functional assessment of rat sciatic nerve regeneration. Neurol Res 26:186–194.
Vergnolle N, Bunnett NW, Sharkey KA, Brussee V, Compton SJ, Grady EF, Cirino G, Gerard N, Basbaum AI, Andrade-Gordon P, Hollenberg MD, Wallace JL (2001) Proteinase-activated receptor-2 and hyperalgesia: a novel pain pathway. Nat Med 7:821–826.
Walker AK, Rivera PD, Wang Q, Chuang JC, Tran S, Osborne-Lawrence S, Estill SJ, Starwalt R, Huntington P, Morlock L, Naidoo J, Williams NS, Ready JM, Eisch AJ, Pieper AA, Zigman JM (2014) The P7C3 class of neuroprotective compounds exerts antidepressant efficacy in mice by increasing hippocampal neurogenesis. Mol Psychiatry.
Wang G, Han T, Nijhawan D, Theodoropoulos P, Naidoo J, Yadavalli S, Mirzaei H, Pieper AA, Ready JM, McKnight SL (2014) P7C3 neuroprotective chemicals function by activating the rate-limiting enzyme in NAD salvage. Cell.
Webb AA, Muir GD (2004) Course of motor recovery following ventrolateral spinal cord injury in the rat. Behav Brain Res 155:55–65.
Wen XJ, Xu SY, Chen ZX, Yang CX, Liang H, Li H (2010) The roles of T-type calcium channel in the development of neuropathic pain following chronic compression of rat dorsal root ganglia. Pharmacology 85:295–300.
Whiteside G, Doyle CA, Hunt SP, Munglani R (1998) Differential time course of neuronal and glial apoptosis in neonatal rat dorsal root ganglia after sciatic nerve axotomy. Eur J Neurosci 10:3400–3408.
Winfree CJ (2005) Peripheral nerve injury evaluation and management. Curr Surg 62:469–476.
Wood MD, Kemp SW, Weber C, Borschel GH, Gordon T (2011) Outcome measures of peripheral nerve regeneration. Ann Anat 193:321–333.
Yin TC, Britt JK, De Jesus-Cortes H, Lu Y, Genova RM, Khan MZ, Voorhees JR, Shao J, Katzman AC, Huntington PJ, Wassink C, McDaniel L, Newell EA, Dutca LM, Naidoo J, Cui H, Bassuk AG, Harper MM, McKnight SL, Ready JM, Pieper AA (2014) P7C3 neuroprotective chemicals block axonal degeneration and preserve function after traumatic brain injury. Cell Rep.
Yoon YW, Na HS, Chung JM (1996) Contributions of injured and intact afferents to neuropathic pain in an experimental rat model. Pain 64:27–36.
Zhao CS, Puurunen K, Schallert T, Sivenius J, Jolkkonen J (2005) Behavioral and histological effects of chronic antipsychotic and antidepressant drug treatment in aged rats with focal ischemic brain injury. Behav Brain Res 158:211–220.

(Accepted 3 October 2014)
(Available online 13 October 2014)